

Multimodal Language and Graph Learning of Adsorption Configuration in Catalysis

Janghoon Ock,[†] Rishikesh Magar,[‡] Akshay Antony,[‡] and Amir Barati Farimani^{*,‡}

[†]*Department of Chemical Engineering, Carnegie Mellon University, 5000 Forbes Street,
Pittsburgh, PA 15213, USA*

[‡]*Department of Mechanical Engineering, Carnegie Mellon University, 5000 Forbes Street,
Pittsburgh, PA 15213, USA*

E-mail: barati@cmu.edu

Abstract

Adsorption energy, a reactivity descriptor, should be accurately assessed for efficient catalyst screening. This evaluation requires determining the lowest energy across various adsorption configurations on the catalytic surface. While graph neural networks (GNNs) have gained popularity as a machine learning approach for computing the energy of catalyst systems, they rely heavily on atomic spatial coordinates and often lack clarity in their interpretations. Recent advancements in language models have broadened their applicability to predicting catalytic properties, allowing us to bypass the complexities of graph representation. These models are adept at handling textual data, making it possible to incorporate observable features in a human-readable format. However, language models encounter challenges in accurately predicting the energy of adsorption configurations, typically showing a high mean absolute error (MAE) of about 0.71 eV. Our study addresses this limitation by introducing a self-supervised multi-modal learning approach, termed graph-assisted pretraining. This method significantly reduces the MAE to 0.35 eV through a combination of data augmentation,

achieving comparable accuracy with DimeNet++ while using 0.4% of its training data size. Furthermore, the Transformer encoder at the core of the language model can provide insights into the feature focus through its attention scores. This analysis shows that our multimodal training effectively redirects the model’s attention toward relevant adsorption configurations from adsorbate-related features, enhancing prediction accuracy and interpretability.

Keywords: Computational Catalysis, Catalyst Screening, Multi-modal Model, Machine Learning, Transformer, Large Language Model

Introduction

Identifying optimal catalyst materials for particular reactions is key to advancing energy storage technology and sustainable chemical processes. The adsorption energy serves as a descriptor in catalyst screening, reflecting a system’s reactivity. Consequently, it often becomes the focal point of both experimental and simulation studies. For this task, labor-intensive experiments or computationally expensive quantum chemistry calculations, such as Density Functional Theory (DFT) simulations, have traditionally been used. The numerous adsorption configurations of an adsorbate on a catalytic surface, which are determined by factors such as adsorption site and adsorbate molecule orientation, pose a significant challenge in determining adsorption energy by solely using expensive DFT calculations.

In our study, we use the term “configuration energy” (ΔE_i) to represent the amount of energy required for the adsorbate to adsorb on the catalytic surface with a specific adsorption configuration, i .¹ The configuration energy is obtained by subtracting the sum of energies of the clean catalytic surface (E_{slab}) and the gas-phase adsorbate molecule (E_{gas}) from the energy of the adsorbate-catalyst system in a specific configuration ($E_{\text{sys},i}$). This process identifies the adsorption energy (ΔE_{ads}) as the minimum energy across all possible configurations in the adsorbate-catalyst combination:

$$\Delta E_i = E_{\text{sys},i} - E_{\text{slab}} - E_{\text{gas}} \quad (1a)$$

$$\Delta E_{\text{ads}} = \min_i(\Delta E_i) \quad (1b)$$

Initial adsorption configurations are typically set using atomic simulation packages such as CatKit² and Pymatgen.³ These configurations are then subjected to DFT calculations, which relax the structures and evaluate their energy levels. Despite the effectiveness of this approach, the high computational demand of DFT simulations restricts their feasibility for analyzing a large number of systems.^{4,5} This bottleneck in practicality necessitates alternative methods.

Machine learning (ML) approaches have emerged as efficient surrogates to DFT simulations, enhancing the speed of adsorption energy predictions.⁶⁻⁸ Lan et al.⁹ proposed a hybrid DFT-ML technique, where ML models initially relax the adsorbate-catalyst system before DFT calculations refine the energy assessment. This method has achieved a 2000-fold increase in speed while maintaining an 87.4% success rate in identifying minimum energy configurations compared to a DFT-only approach. The importance of such techniques has drawn attention beyond the chemical engineering and chemistry communities, extending into the AI4Science field. This interest was highlighted by MetaAI’s hosting of the Open Catalyst Challenge 2023 at the NeurIPS workshop, which focused on utilizing advanced ML models for determining adsorption energy.¹⁰

Graph Neural Networks (GNNs) serve as primary ML models in these hybrid approaches. Their ability to effectively capture the complexities of atomic structures accounts for their high performance in predicting energy and interatomic forces. Converting 3D coordinates into graph representations requires a precise understanding of spatial information. This conversion is conducted based on the identification of nearest neighbors within specific proximity thresholds for each atom. However, achieving such precise coordinates can be challenging,

particularly when working with experimental results. This difficulty can limit the effectiveness of the early-stage catalyst screening process and create a disconnect between experiments and simulations. Moreover, the inherently complex nature of graph representations adds another layer of challenge, as these representations are less intuitive for human interpretation.^{11,12} This complexity blocks the straightforward integration of observable features into the model’s input.

Using language-based representations serves as an effective alternative to graph representations, allowing for the incorporation of observable features in a format that is easier for human understanding. Additionally, from the modeling perspective, we often possess metadata that includes specific observable attributes, such as bulk composition, bulk structure type, and surface orientation.⁸ In this context, using the metadata information could be more advantageous and practical than depending exclusively on the graph representation which is sourced from atomic structures. Moreover, the recent advancements in the field of natural language processing, particularly with the rise of Transformer models, have extended their application to chemistry, biology, and materials science. The use of Transformer-based language models in these domains has grown in popularity, as evidenced by references such as ChemBERTa,¹³ SMILES-BERT,¹⁴ GPCR-BERT,¹⁵ PeptideBERT,¹⁶ TransPolymer,¹⁷ and MOFormer.¹⁸

In the catalysis research field, our prior research¹⁹ introduced the CatBERTa model, which utilizes a language model-based approach for predicting adsorbate-catalyst properties. Employing the RoBERTa encoder,²⁰ originally developed for language processing, CatBERTa effectively processes textual inputs. This enables the model to work exclusively with textual data, such as text strings and natural language descriptions. CatBERTa demonstrates accuracy comparable to earlier GNNs, achieving a mean absolute error (MAE) of 0.7-0.8 eV in predicting the relaxed energy from their initial structures. However, CatBERTa’s current accuracy level poses challenges in precisely identifying subtle variations in configuration energy, especially for the same adsorbate-catalyst pairs where energy differences are marginal.

Our study introduces graph-assisted pretraining, a multi-modal learning method that uses both graph and text modalities to improve prediction accuracy for adsorption configurations. The aim of graph-assisted pretraining is to transfer knowledge captured in graph embeddings to text embeddings, thus enriching the text embedding. In addition, we present configuration augmentation, an efficient data augmentation strategy designed to expose the model to a wide range of adsorption configurations. Configuration augmentation can be used independently or in conjunction with graph-assisted pretraining, offering flexibility in application based on the data availability scenario.

Results and discussion

Framework

The language model developed for catalyst property prediction utilizes textual data to estimate the relaxed energy of the adsorbate-catalyst system, as illustrated in Figure 1. The textual input is derived from the relaxed structures in the Open Catalyst 2020 (OC20) and Open Catalyst 2020 Dense (OC20-Dense) datasets. Our study employs the CatBERTa model, a pioneering language model-based approach for predicting catalyst properties. To enhance the CatBERTa model’s accuracy for adsorption configurations, we have established a multi-modal training framework called graph-assisted pretraining. This framework leverages both text and graph modalities in a self-supervised manner during pretraining. The process then advances to a fine-tuning stage, where the model is trained in a supervised manner using energy labels calculated through DFT.

The CatBERTa model solely relies on textual input, which can range from textual strings to natural language descriptions. In this paper, we opt for the textual string format, which demonstrated the highest predictive accuracy in the initial CatBERTa study. Our framework’s goal is to predict the energy of a relaxed configuration based on its corresponding relaxed structure, using textual strings from DFT-relaxed structures. These strings are gen-

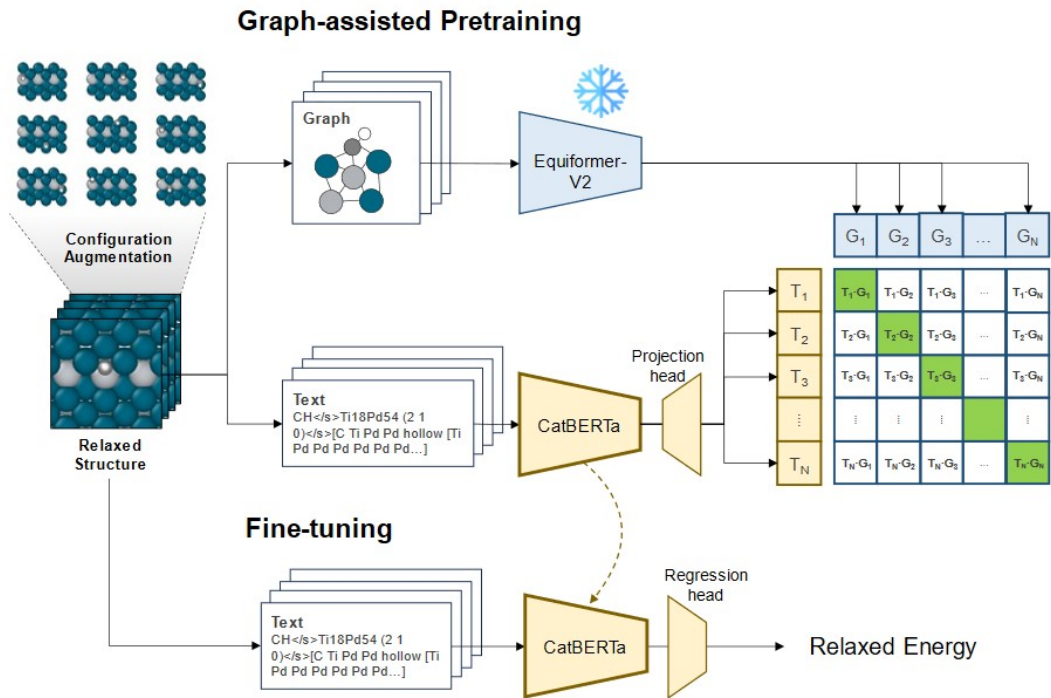


Figure 1: Overview of the enhancement strategies.

erated by converting relaxed structures into textual data, as shown in Figure 2(a). This conversion employs metadata from the OC20 and OC20-Dense datasets, including adsorbate and catalyst symbols and surface orientation, and uses Pymatgen to identify interacting atoms. Further details on this structure-text conversion process and dataset application are available in the Methods section.

In our methodology, both training and validation are conducted using DFT-relaxed structures, while our predictions are made on ML-relaxed structures. The rationale for this approach is grounded in the nature of DFT relaxation, which not only yields the relaxed structure but also directly provides the relaxed energy. Utilizing DFT relaxation for obtaining structures and then predicting their energies would be redundant and inefficient. To circumvent this, we apply the CatBERTa model to ML-relaxed structures, aligning with a more practical ML approach. These ML-relaxed structures, along with their DFT-calculated energies, are provided by the Open Catalyst Project Challenge 2023. The ML relaxation utilized models such as GemNet-OC, SCN, and eSCN. Our model’s accuracy is evaluated

on 920 ML-relaxed structures that have valid DFT energies. We quantify the uncertainty of our model’s predictions by calculating the standard deviation across predictions for structures relaxed using GemNet-OC, SCN, and eSCN. We conduct embedding and attention score analysis using the entire set of ML-relaxed structures, which encompasses a range from 11,508 to 11,755. This analysis is performed irrespective of whether these structures have verified DFT energies.

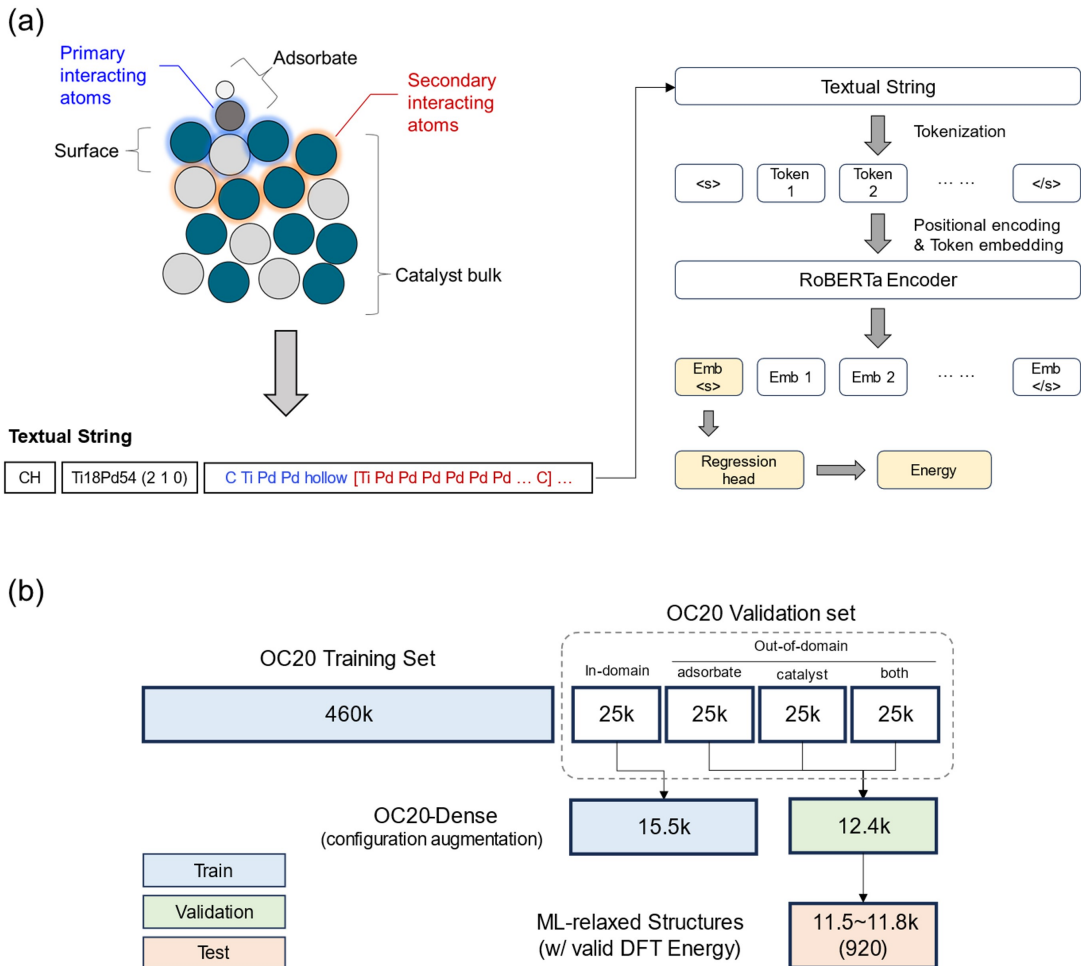


Figure 2: Model training process. **a** Illustrative depiction of structure-text conversion and its integration into CatBERTa. The textual string comprises three sections: adsorbate, catalyst, and adsorption configuration. **b** Dataset utilization for training, validation, and testing.

Graph-assisted pretraining, a core component of our framework, is designed to enable knowledge transfer from graph embeddings to text embeddings. We select EquiformerV2 as

a graph encoder since it shows excellent performance with the OC20 dataset.^{21,22} The CatBERTa model serves as a text encoder, producing text embeddings. These text embeddings are then projected to match the dimensions of the graph embeddings. A contrastive loss is applied to increase the similarity between these two types of embeddings, with the graph encoder frozen. This approach is inspired by the contrastive language-image pretraining (CLIP) method.²³

To further improve the model’s accuracy, we implemented configuration augmentation, a targeted data augmentation strategy focusing on improving the model’s understanding of adsorption configurations. This method extracts additional data from the OC20-Dense dataset, where adsorption configurations are abundant, as opposed to the OC20 dataset. our validation and test sets consist exclusively of unencountered adsorbates and catalysts, as depicted in Figure2(b). By exclusively using the in-domain (ID) split in the OC20-Dense dataset, we can ensure that the improved prediction accuracy of the test set is not because of the increased exposure to originally unseen adsorbate and catalyst. The addition of 15,450 data from the in-domain split of the OC20-Dense, constituting merely 3.3% of the entire OC20 dataset, significantly elevates the model’s accuracy. This is achieved by making the model familiar with a broader range of adsorption configurations. This data augmentation can be applied either exclusively or in conjunction with graph-assisted pretraining.

Accuracy improvement

The proposed multimodal pretraining method effectively improves the accuracy of configuration energy predictions, as shown in Table S2. This method incorporates graph modality exclusively during the pretraining phase, leaving the fine-tuning process identical to that of the standard CatBERTa approach. The graph-assisted pretraining achieves a substantial 9.7% decrease in MAE. This improvement is further enhanced when combined with configuration augmentation leading to a remarkable MAE reduction to 0.35 eV—a 51.5% decrease compared to the baseline. Even when compared to cases using only configuration augmen-

tation, the method presents an additional 8.5% reduction in MAE. These improvements are also reflected in the increased R^2 values and visualized in the parity plots in Figure 3.

When graph modality data are not obtainable, applying configuration augmentation alone is a feasible option. The exclusive use of configuration augmentation leads to a 47.0% reduction in MAE relative to the baseline case. Furthermore, this approach considerably diminishes the uncertainty across different ML-relaxed structures. Specifically, it reduces the uncertainty to less than one-third compared to cases without configuration augmentation. This demonstrates that configuration augmentation not only enhances the accuracy of predictions but also ensures greater stability and reliability of predictions derived from various ML relaxations.

Table 1: Performance comparison of CatBERTa with enhancements, including graph-assisted pretraining (GAP) and configuration augmentation (CA). The training times for DimeNet++, GemNet-OC, and EquiformerV2 are measured on V100 GPUs,²² while CatBERTa’s training time is based on the A6000 GPU. Direct comparison of training times is challenging due to these different GPU environments. Although the A6000 GPU is known to be approximately 12–50% faster than the V100,^{24,25} CatBERTa’s training duration is notably shorter in comparison to the other models.

Model	Enhancement	Training data size	Training time [GPU-days] (↓)	Prediction results		Improvement (vs. CatBERTa _{baseline})	
				MAE [eV] (↓)	R^2 [-] (↑)	MAE (↓)	R^2 (↑)
CatBERTa	baseline	460k	0.31	0.713 ± 0.014	0.584 ± 0.014	0.00%	0.000
	GAP	460k	0.53	0.643 ± 0.020	0.691 ± 0.015	-9.73%	+0.108
	CA	476k	1.14	0.378 ± 0.005	0.863 ± 0.005	-46.96%	+0.279
	GAP+CA	476k	0.68	0.346 ± 0.005	0.882 ± 0.002	-51.50%	+0.298
DimeNet++	-	134M	1600	0.326 ± 0.007	0.894 ± 0.004	-	-
GemNet-OC	-	134M	765	0.177 ± 0.028	0.953 ± 0.012	-	-
EquiformerV2	-	134M	705	0.132 ± 0.003	0.971 ± 0.001	-	-

While the enhanced accuracy of CatBERTa has not yet reached the levels of state-of-the-art GNN or Transformer models that utilize graph representations, its performance is comparable to that of DimeNet++. It is important to acknowledge that these GNN models have undergone extensive training with approximately 134 million data points, which resulted in significant training time, as detailed in Table S2. Given the disparity in the volume of training data, it is impractical to directly compare the inherent predictive capabilities of models such as DimeNet++, GemNet-OC, EquiformerV2, and CatBERTa. Additionally, the use of language models for atomic property prediction is a relatively new approach com-

pared to graph representation-based methods.^{26–28} Specifically, the application of language models for predicting adsorbate-catalyst systems was first introduced in 2023.¹⁹ Considering this context, it is noteworthy that our enhancement strategies can bring the accuracy of CatBERTa close to that of DimeNet++ with merely about 0.4% of the data size. This underscores the promising opportunity for further refining the accuracy of language models in atomic property prediction, potentially expanding their applicability in this domain.

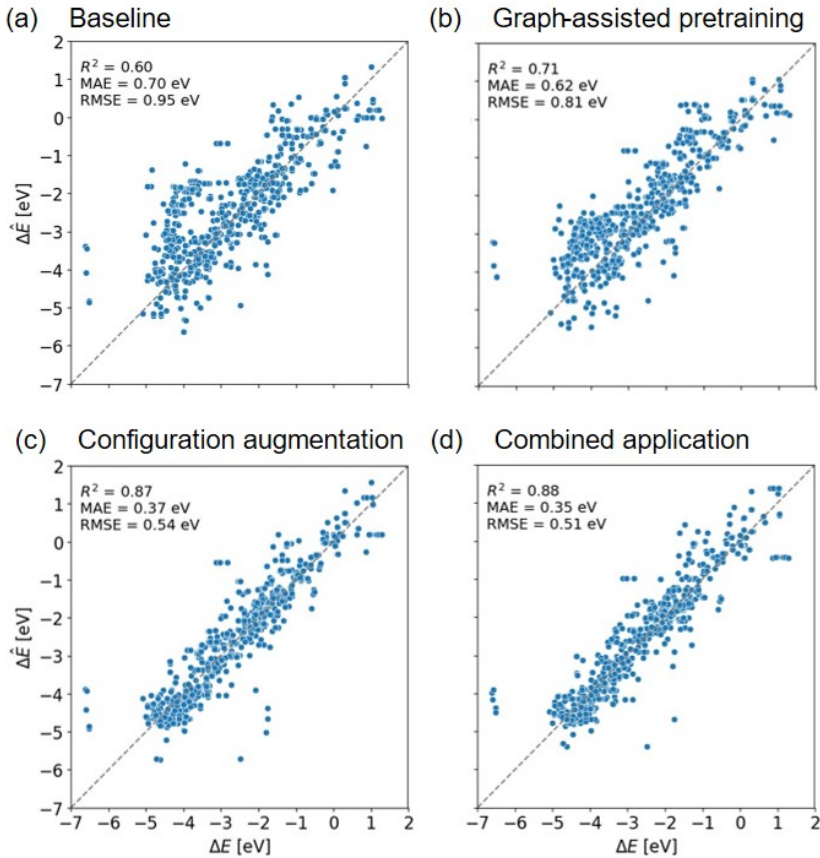


Figure 3: Parity plots comparing DFT-calculated (x-axis) and CatBERTa-predicted (y-axis) energy values on structures relaxed using GemNet-OC. All subfigures are aligned with identical x and y-axes for direct comparison. **a** The baseline model without enhancements. **b** Graph-assisted pretraining. **c** Configuration augmentation. **d** The combined application of both enhancements.

Sectional attention scores

The analysis of attention scores in the final layer, corresponding to different sections, offers insights into how attention is allocated during the energy prediction process. We extract and average the attention scores for the “<s>” token, fed to the regression head, between other tokens across three distinct sections: the adsorbate, the catalyst, and the adsorption configuration (see Figure2(b)). This method aids in deciphering the model’s focus for each section. In addition, we compute the attention score of the special “<s>” token with respect to itself. The section-wise averaged attention scores are presented in Table 2.

Table 2: Attention scores between the “<s>” token and other tokens in each section of the textual string. These scores are computed from the final hidden layer and are averaged across all 12 attention heads. The “<s>” column represents self-attention score between “<s>” token and itself.

Enhancement	Average attention score			
	<s>	Adsorbate	Catalyst	Configuration
baseline	0.05	0.45	0.15	0.35
GAP	0.01	0.15	0.30	0.54
CA	0.03	0.08	0.36	0.53
GAP+CA	0.02	0.20	0.18	0.60

In the three enhanced cases, attention scores for the adsorption configuration section show a significant increase compared to the baseline case. These cases also reveal a shift in the model’s focus: while the baseline CatBERTa concentrates mainly on the adsorbate section, enhancements strategies reallocate this focus towards both the catalyst and configuration sections. This shift in the model’s attention aligns with the physical principle that the interaction of the adsorbate with the catalytic surface as a whole is more critical than analyzing the adsorbate and the surface as separate entities.^{29,30} Supporting this view, the combined use of both graph-assisted pretraining and configuration augmentation results in the most significant attention being directed to the configuration section across all scenarios. This finding highlights the effectiveness of these strategies in accurately modeling the interactions between the adsorbate and the catalyst.

These preliminary observations shed light on the model’s prioritization of specific features. Nevertheless, it is crucial to acknowledge that attention scores might not fully encapsulate the interaction dynamics between tokens and their impact on prediction outcomes, especially since the evaluation overlooks the role of value matrices.³¹ We acknowledge that fully unraveling the intricacies of interpreting attention scores requires further in-depth study.

Duplicate text sets

Our textual representation, which relies on interacting atoms to depict adsorption configurations, is less sophisticated than a graph representation in capturing structural nuances in similar configurations. This is illustrated in Figure 4(a), where the provided structures exhibit subtle differences that are difficult to discern visually. The graph representation successfully captures these nuances, leading to similar yet distinct configuration energy values for each structure, which range from -2.06 to -2.01 eV. In contrast, our textual representation does not discern these subtle differences, producing identical textual strings for all five structures. Consequently, this leads to identical energy predictions across these structures.

The inaccuracy of the CatBERTa model is primarily due to duplicate texts representing different structures. “Duplicate text sets” refer to those that present the same text for different structures, while “unique text sets” represent those with no duplicates. As shown in Figure 4(b), in the baseline case, the duplicate text sets exhibit approximately 40% higher MAE compared to the unique text sets. When an enhancement strategy is implemented, the accuracy for the duplicate sets improves. This suggests that even though textual representations for duplicate sets do not capture subtle structural differences, their overall prediction accuracy can be enhanced by our enhancement strategy. This observation suggests that refining the textual string to generate distinct texts for similar adsorption configurations could improve CatBERTa’s accuracy.

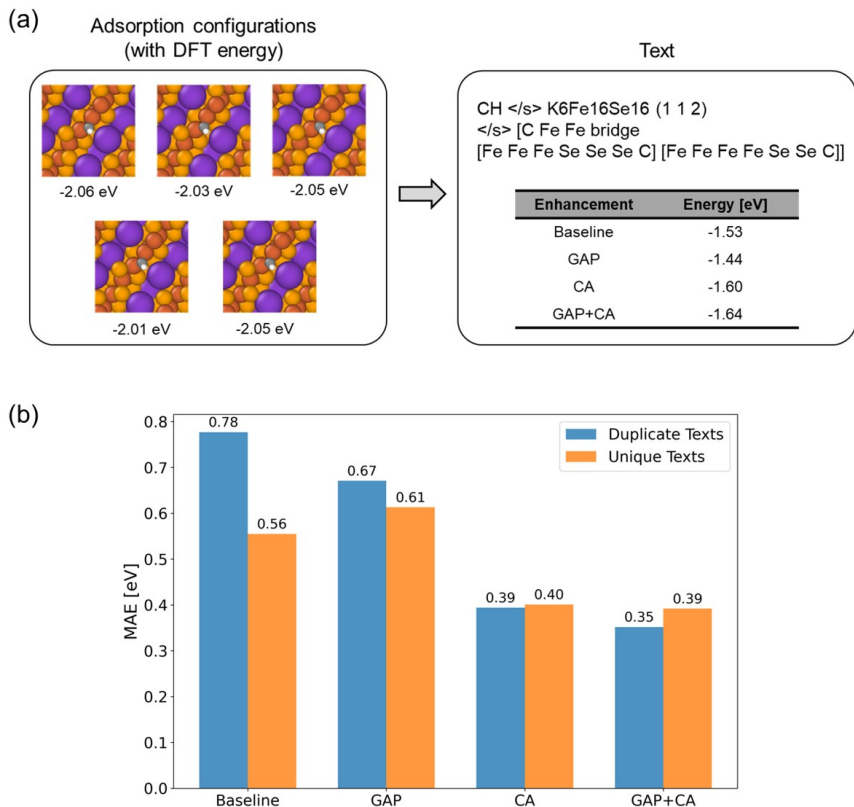


Figure 4: Comparative analysis of prediction performance on duplicate and unique text sets. **a** Instances illustrating the limitation of our textual approach in distinguishing minor structural differences. **b** MAE for each subset, comparing baseline scenarios to cases with enhancements applied. Visual representations through parity plots are available in the supplementary material, Figure S1.

Graph-assisted pretraining

Graph-assisted pretraining aims to transfer knowledge from graphs to text embeddings, ensuring that text embeddings resemble graph embeddings. The embeddings are extracted after the final layer normalization, which precedes the energy and force prediction stage, as illustrated in Figure 5. Within this model, each atom is represented as a node, and each atom node is characterized by a two-dimensional embedding tensor, collectively forming a three-dimensional tensor for the entire system. The size of the system tensor is defined by the number of atoms, the count of spherical channels, and the maximum degree of spherical harmonics involved.²² The extraction of graph embeddings begins with reshaping the two-dimensional atom embedding tensor into a one-dimensional tensor. Subsequently, max-

pooling is applied across all these one-dimensional atom embeddings in the system, yielding a single, comprehensive embedding for each system. In our study, the final embedding of each system is represented by a tensor with a size of 3,200. Consequently, during the graph-assisted pretraining phase, text embeddings, initially sized at 768, undergo a linear projection head to match the 3,200-size tensor.

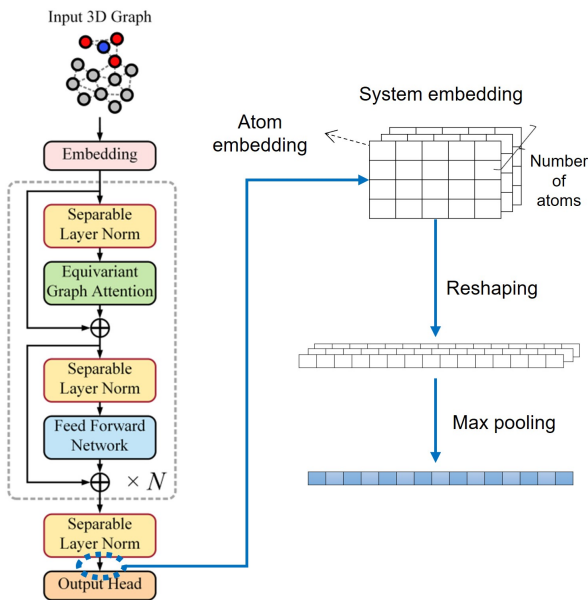


Figure 5: Schematic for obtaining a representative EquiformerV2 embedding for a specific system. The left architecture image is taken from the original EquiformerV2 paper.²²

Table 3 outlines the pretraining and fine-tuning methods for each enhancement case. The baseline CatBERTa model uses a RoBERTa encoder, initially pretrained on a massive English corpus, with masked language modeling for natural language processing tasks.^{19,20} Following this, the model undergoes fine-tuning for an energy prediction task. To elucidate the effects of graph-assisted pretraining, we present a comparative analysis using t-SNE visualizations in Figure 6. These visualizations contrast the max-pooled EquiformerV2 embeddings, embeddings derived from masked language modeling, and embeddings from graph-assisted pretraining. The EquiformerV2 embeddings, serving as the graph embeddings, guide the text encoder embeddings within the graph-assisted pretraining. For the latter two cases, we analyze the t-SNE of the “<s>” token embeddings from the encoder, which are extracted

before being processed through the regression or projection head. These embeddings depict the initial state of the latent space prior to fine-tuning. The embeddings generated through masked language modeling represent the starting point for the baseline CatBERTa model.

Table 3: CatBERTa pretraining approaches. Data obtained from the OC20 and OC20-Dense datasets originate from the relaxed structures produced by each DFT relaxation.

Enhancement	Pretraining		Fine-tuning	
	Method	Data Source	Method	Data Source
baseline	Masked language modeling	English corpus	Energy prediction	OC20
GAP	Graph-assisted pretraining	OC20	Energy prediction	OC20
CA	Masked language modeling	English corpus	Energy prediction	OC20 & OC20-Dense
GAP+CA	Graph-assisted pretraining	OC20 & OC20-Dense	Energy prediction	OC20 & OC20-Dense

Our findings demonstrate that graph-assisted pretraining is relatively more effective in clustering systems in the latent space according to their energy levels and adsorbate types, compared to the encoder pretrained with masked language modeling. In Figure 6, the EquiformerV2 embeddings (panels a and d) exhibit distinct clustering for systems with low configuration energy and identical adsorbate types, exemplifying an ideal latent space organization. We presume this clustering precision is associated with the high accuracy of EquiformerV2 in energy predictions. Conversely, the encoder pretrained with masked language modeling results in a more scattered distribution of embeddings (panels b and e), though some degree of clustering exists. Systems with lower configuration energy and nitrogen-containing adsorbates show more pronounced clustering in graph-assisted pretraining, compared to the masked language modeling approach (comparing panels b and c, e and f, respectively). Consequently, graph-assisted pretraining restructures the latent space to reflect the high-performance traits of EquiformerV2, thereby providing a more effective starting point for the subsequent fine-tuning process.

Configuration augmentation

The primary goal of configuration augmentation is to expose the model to a diverse range of adsorption configurations within the training dataset, enabling the model to discern subtle

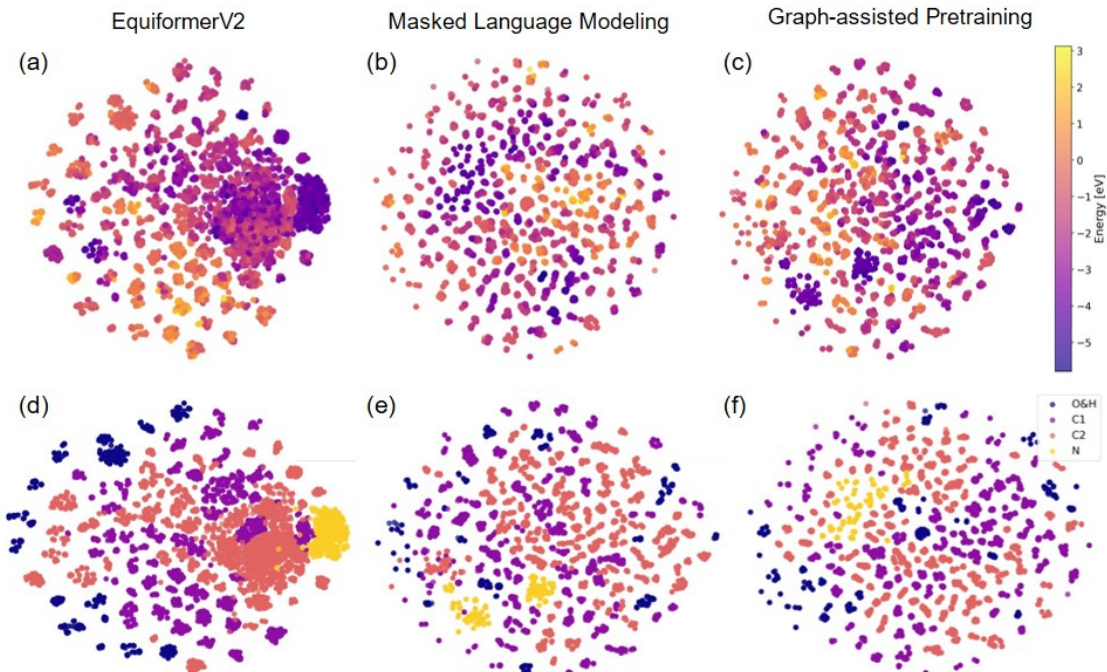


Figure 6: t-SNE visualizations of graph and text embeddings. Graph embeddings are derived from EquiformerV2, while text embeddings are from CatBERTa’s “<s>” token. Upper row panels **a-c** use colors to indicate configuration energy levels, while lower row panels **d-f** color-code by adsorbate type. These adsorbate types are represented as follows: O&H (oxygen/hydrogen), C1 (single carbon-containing adsorbates), C2 (two carbon-containing adsorbates), and N (nitrogen-containing adsorbates)

variations in these configurations. This augmentation can be applied to the downstream fine-tuning step and pretraining step. Our proposed approach utilizes the final frames of relaxation trajectories from the OC20-Dense dataset as an augmentation dataset. This method can achieve nearly a 47.0% reduction in MAE by incorporating augmentation data that constitutes only 3.3% of the main training dataset from OC20. It is important to note that this approach maintains the integrity of the test set. Since the OC20-Dense training set originates from an in-domain split of the OC20 validation dataset, the test set, derived from the out-of-domain split of the OC20 validation dataset, remains a collection of unseen adsorbate and catalyst combinations, even after adding the augmentation data.

To assess the effectiveness of our configuration augmentation method, we conduct a comparative analysis using a dataset where the augmented data is sourced from intermediate

Table 4: Comparison of data augmentation methods. The method involving configuration augmentation with OC20-Dense relaxed data is denoted as “CA”. In contrast, the comparison case, labeled “CA_{int}”, conducts random sampling of intermediate structures from the OC20 relaxation trajectories.

Enhancement	Main Data (size)	Augmentation Data (size)	MAE [eV] (\downarrow)	R^2 [-] (\uparrow)
baseline	OC20 relaxed structures (460k)	-	0.713 ± 0.014	0.584 ± 0.014
CA	OC20 relaxed structures (460k)	OC20-Dense relaxed structures (16k)	0.378 ± 0.005	0.863 ± 0.005
CA _{int}	OC20 relaxed structures (460k)	OC20 intermediate structures (16k)	0.861 ± 0.011	0.397 ± 0.013

frames of relaxation trajectories in the OC20 dataset, as shown in Table 4. We incorporate a sample of 15,450 data points, randomly selected from these intermediate frames, into the training dataset. While the volume of augmentation data is the same as that of our proposed configuration augmentation method, the source of the data differs. This comparison case with the intermediate frames results in decreased accuracy. The addition of random intermediate frames proves ineffective in helping the model capture the subtle aspects of relaxed adsorption configurations. On the contrary, the inclusion of relaxed configurations substantially enhances model accuracy, validating the effectiveness of our configuration augmentation method.

Conclusion

The recent adoption of language models in predicting catalytic properties enables a more seamless integration of features into the input data. Nonetheless, the current CatBERTa model shows a limitation in accurately distinguishing subtle variations in adsorption configurations, which is crucial for determining adsorption energy. For the effective application of the language model in computational catalysis, it is essential to enhance the accuracy of these predictions. To address this challenge, we have introduced a multimodal pretraining approach, complemented by an effective data augmentation strategy.

Our graph-assisted pretraining method enhances the accuracy of the language model by guiding the text modality with a high-performing graph modality. This method results in a 9.7% reduction in MAE compared to the baseline CatBERTa. This improvement is achieved

while retaining the same fine-tuning process as the text-only baseline model, demonstrating the method’s effectiveness. The key to this accuracy improvement lies in making the fine-tuning step start with a more informed latent space. Additionally, when the graph-assisted pretraining is complemented with configuration augmentation, there is a further reduction in MAE by 51.5%, highlighting the effectiveness of this combined approach.

Our findings also reveal a limitation in the current textual representation: its struggle to discern very subtle structural differences. This limitation is a major hurdle in accurately predicting energy using text. This insight directs future research toward refining the textual representation for adsorbate-catalyst systems. The refinement should focus on the description of the adsorption configuration. This is because our analysis of attention scores indicates that understanding features related to the adsorption configuration is more crucial for accurate energy modeling than focusing solely on individual adsorbate and catalyst information.

In our research, we load a high-performing public checkpoint into the graph encoder and freeze it during the pretraining step. This approach allows the graph embedding to act as guidance for the text modality during the training phase. However, unlocking the graph encoder and training both encoders concurrently could promote advanced cross-modal learning, enabling the model to gain a deeper understanding of both modalities. Such a strategy is expected to be highly effective, especially after the textual representation has been refined to capture the intricate nuances of similar systems. A sophisticated textual representation can provide additional insights, complementing those from the graph representation. This comprehensive approach to cross-modal learning, which has already shown success in fields like symbolic regression³² and computer vision,²³ holds great promise for enhancing the predictive ability of our language model.

Methods

Open Catalyst dataset

The OC20 dataset stands as the most extensive and varied dataset for heterogeneous catalysts. It encompasses over 1.2 million DFT relaxations, all using the revised Perdew-Burke-Ernzerhof (RPBE) functional.^{8,33} This dataset features various tasks, including Initial-Structure-to-Energy (IS2RE), Initial-Structure-to-Relaxed-Structure (IS2RS), and Structure-to-Energy-and-Force (S2EF). In our study, we focus on the data for the IS2RE/IS2RS task, which consists of 460,328 DFT relaxations. Our objective is to predict the configuration energy based on the relaxed structure, which leads us to specifically select the last frame of these relaxation trajectories. In Table S2, the benchmark cases for DimeNet++, GemNet-OC, and EquiformerV2 were trained on the S2EF task dataset, which comprises 133,934,018 frames from DFT relaxations.

To investigate the global minimum energy, also known as the adsorption energy, of adsorbate-catalyst combinations, the OC20-Dense dataset was developed.⁹ The OC20 dataset, while extensive in types of adsorbates and catalytic surfaces, lacks variation in adsorption configurations. OC20-Dense dataset addresses this by densely enumerating these configurations. The initial configurations of adsorbates on surfaces are produced using both heuristic and random approaches.^{2,3,9} These configurations then undergo relaxations using both ML and DFT methods. The OC20-Dense dataset contains 995 distinct adsorbate-catalyst combinations, evenly selected from the in-domain and three out-of-domain splits, from the OC20 validation set (see Figure 2(b)). For our research, we conform to the training and validation data splits set provided by the Open Catalyst Challenge 2023.¹⁰ The training set for the OC20-Dense, drawn from the in-domain split of the OC20 validation set, comprises 15,450 data entries. We utilize this dataset specifically for configuration augmentation. The validation set for the OC20-Dense is created by randomly selecting 12,372 data entries from its three out-of-domain splits.

As part of the Open Catalyst Challenge 2023, the Open Catalyst Project has provided a set of ML-relaxed structures along with their energies calculated using DFT. These structures, originating from the OC20-Dense validation set and illustrated in Figure 2(b), were relaxed using models like GemNet-OC, SCN, and eSCN. Any relaxed structures that are invalid or lack valid DFT energy values are excluded. This includes cases where the adsorbate fails to bind to the surface, decomposes into different atoms or molecules, or causes significant alterations to the surface from its original state. After filtering out these invalid configurations, the remaining counts for the ML-relaxed test sets using the GemNet-OC, SCN, and eSCN models are 11,508, 11,630, and 11,755 structures, respectively. Within these datasets, only a subset of structures—919, 922, and 922 respectively—have valid DFT-verified energy values. Our accuracy analysis concentrates on these approximately 920 ML-relaxed structures, each supported by a reliable DFT energy assessment. Meanwhile, the embedding and attention score analyses fully utilize predictions on all the valid ML-relaxed structures.

Textual string generation

The input data is entirely text-based, adhering to the string-type input format outlined in the original CatBERTa paper.¹⁹ We generate textual strings by converting the relaxed structures in the OC20 and OC20-Dense datasets, as illustrated in Figure 2(a). Our textual input format is structured into three segments: the adsorbate, the catalytic surface, and the depiction of the adsorption configuration. Specifically, the adsorbate segment simply contains its elemental symbol. For the catalytic surface part, we integrate information about the catalyst’s overall composition along with its Miller index. For these two segments, the information is sourced from the pre-existing metadata of the OC20 dataset. The depiction of the adsorption configuration is achieved by pinpointing both the primary and secondary atoms involved in the interaction. This method is selected due to its proven effectiveness in predicting energy outcomes in previous research.¹⁹ In this process, we identify these interacting elements by using the Pymatgen. First, we establish atomic connectivity based on a

predefined cutoff radius. Then, we pinpoint the atoms connected to those in the adsorbate and surface. The connected atoms of the adsorbate atoms are classified as primary interacting atoms, while the neighboring atoms of the primary interacting atoms on the surface are grouped as secondary interacting atoms.

CatBERTa

In this research, we employ the CatBERTa model as a representative language model. This text-based model is specifically designed and trained for predicting relaxed energy in adsorbate-catalyst systems. The model incorporates the RoBERTa encoder, originally pre-trained on an extensive natural language corpus that includes resources such as BookCorpus and English Wikipedia, cumulatively exceeding 160GB.²⁰ The RoBERTa, diverging from the conventional BERT model³⁴ which masks a fixed 15% of tokens in each epoch during training, adopts a dynamic masking approach. This method alters the masked tokens variably across different training epochs, thereby improving the model’s proficiency in predicting masked words and grasping syntactic and semantic nuances.

The CatBERTa model is fine-tuned for an energy prediction task. The original RoBERTa’s classification head is replaced with a regression head, comprising a linear and activation layer. This modification allows CatBERTa to generate a singular scalar value of energy predictions. For this prediction, the embedding of the special “<s>” token, after encoder processing, serves as input for this regression head. The training hyperparameters and the architecture details of the CatBERTa model are provided in Table S1.

EquiformerV2

The Equiformer is a GNN which is SE(3)/E(3)-equivariant, adeptly fusing the inductive biases of equivariance with the dynamic strengths of Transformers.²¹ The Equiformer stands out by demonstrating that Transformers can, in fact, be effectively adapted to 3D atomistic graphs. This is achieved by two main factors. To begin, the Equiformer modifies the

traditional Transformer by substituting SE(3)/E(3)-equivariant operations for the original operations. Second, the Equiformer model introduces equivariant graph attention, a novel attention mechanism.

In the pretraining stage, we utilize the EquiformerV2 embedding for graph representation purposes due to its excellent performance in the OC20 dataset. The EquiformerV2, a refined version of the original Equiformer, brings to the table a host of enhancements. These improvements encompass the replacement of SO(3) convolutions with eSCN convolutions, the introduction of attention re-normalization, the incorporation of separable S2 activation, and the application of separable layer normalization.²² Such advancements have elevated the EquiformerV2, especially in the task of energy and force predictions on the OC20 dataset. The model demonstrates state-of-the-art accuracy in its performance, achieving an MAE of 0.22 eV for the S2EF task and 0.31 eV for the IS2RE task, outperforming other benchmarked models.

Contrastive pretraining

Graph-assisted pretraining synergistically combines text and graph modalities through a self-supervised framework. Utilizing the graph encoder EquiformerV2 in a static (frozen) state, this method is specifically designed to facilitate the transfer of insights from the graph representations to the text modality.

Inspired by the methodology used in Contrastive Language-Image Pretraining (CLIP),²³ this graph-assisted pretraining strategy incorporates both text and graph encoders. The pretraining mechanism is centered around the optimization of a symmetric cross-entropy loss.³⁵ This optimization is mainly dependent on the similarity scores derived from pairs of text and graph embeddings. In this context, a contrastive loss function is used with the primary objective of forging a meaningful correlation between these text and graph embeddings. The overarching aim is to ensure the precise alignment of embeddings from corresponding text-graph pairs, while also effectively differentiating between those pairs that

do not correspond.

The mathematical formulation of the loss function is defined as follows:

$$L = -\frac{1}{N} \sum_{i=1}^N \log \frac{e^{\text{sim}(G_i, T_i)/\tau}}{\sum_{j=1}^N e^{\text{sim}(G_i, T_j)/\tau}} - \frac{1}{N} \sum_{i=1}^N \log \frac{e^{\text{sim}(T_i, G_i)/\tau}}{\sum_{j=1}^N e^{\text{sim}(T_i, G_j)/\tau}}, \quad (2)$$

In this expression, T_i and G_i represent the embeddings of the i -th text and graph, respectively. The function $\text{sim}(G_i, T_j)$ calculates the cosine similarity between the embeddings of the i -th graph and j -th text. Additionally, τ is introduced as a temperature parameter, serving to appropriately scale the similarity scores within the model.

Supporting Information Available

Hyperparameters and architecture of CatBERTa, results from diverse ML-relaxed structures, prediction results of duplicate text sets

Acknowledgement

The authors acknowledge the Bradford and Diane Smith Fellowship for their pivotal funding support.

Technology Use Disclosure

ChatGPT was used to help prepare the preprint version of this manuscript, specifically for grammar and typo corrections. All information in this manuscript has been read, corrected, and verified by all authors.

Data Availability Statement

Access to the Open Catalyst 2020 dataset is provided via this link: <https://github.com/Open-Catalyst-Project/ocp>. The Open Catalyst 2020 Dense dataset and relevant data pertaining to the Open Catalyst Challenge 2023 are available at: <https://github.com/Open-Catalyst-Project/AdsorbML>.

Code Availability Statement

The Python code employed in this study is available on GitHub at the following link: <https://github.com/hoon-ock/multi-view>.

References

- (1) Ock, J.; Tian, T.; Kitchin, J.; Ulissi, Z. Beyond independent error assumptions in large GNN atomistic models. *The Journal of Chemical Physics* **2023**, *158*, 214702.
- (2) Boes, J. R.; Mamun, O.; Winther, K.; Bligaard, T. Graph Theory Approach to High-Throughput Surface Adsorption Structure Generation. *The Journal of Physical Chemistry A* **2019**, *123*, 2281–2285.
- (3) Ong, S. P.; Richards, W. D.; Jain, A.; Hautier, G.; Kocher, M.; Cholia, S.; Gunter, D.; Chevrier, V. L.; Persson, K. A.; Ceder, G. Python Materials Genomics (Pymatgen): A Robust, Open-source Python Library for Materials Analysis. *Computational Materials Science* **2013**, *68*, 314–319.
- (4) Wander, B.; Broderick, K.; Ulissi, Z. W. Catlas: an automated framework for catalyst discovery demonstrated for direct syngas conversion. *Catal. Sci. Technol.* **2022**, *12*, 6256–6267.

- (5) Tran, R.; Wang, D.; Kingsbury, R.; Palizhati, A.; Persson, K. A.; Jain, A.; Ulissi, Z. W. Screening of bimetallic electrocatalysts for water purification with machine learning. *The Journal of Chemical Physics* **2022**, *157*, 074102.
- (6) Goldsmith, B. R.; Esterhuizen, J.; Liu, J.-X.; Bartel, C. J.; Sutton, C. Machine Learning for Heterogeneous Catalyst Design and Discovery. *AIChE Journal* **2018**, *64*, 2311–2323.
- (7) Zitnick, C. L. et al. An Introduction to Electrocatalyst Design using Machine Learning for Renewable Energy Storage. 2020; <https://arxiv.org/abs/2010.09435>.
- (8) Chanussot, L. et al. Open Catalyst 2020 (OC20) Dataset and Community Challenges. *ACS Catalysis* **2021**, *11*, 6059–6072.
- (9) Lan, J.; Palizhati, A.; Shuaibi, M.; Wood, B. M.; Wander, B.; Das, A.; Uyttendaele, M.; Zitnick, C. L.; Ulissi, Z. W. AdsorbML: a leap in efficiency for adsorption energy calculations using generalizable machine learning potentials. *npj Computational Materials* **2023**, *9*, 172.
- (10) Open Catalyst Challenge. <https://opencatalystproject.org/challenge.html>, 2023; Accessed: December 24, 2023.
- (11) Ju, W.; Fang, Z.; Gu, Y.; Liu, Z.; Long, Q.; Qiao, Z.; Qin, Y.; Shen, J.; Sun, F.; Xiao, Z.; Yang, J.; Yuan, J.; Zhao, Y.; Luo, X.; Zhang, M. A Comprehensive Survey on Deep Graph Representation Learning. 2023; <https://arxiv.org/abs/2304.05055>.
- (12) Scafarto, G.; Ciortan, M.; Tihon, S.; Ferre, Q. Augment to Interpret: Unsupervised and Inherently Interpretable Graph Embeddings. 2023; <https://arxiv.org/abs/2309.16564>.
- (13) Chithrananda, S.; Grand, G.; Ramsundar, B. ChemBERTa: Large-Scale Self-Supervised Pretraining for Molecular Property Prediction. 2020; <https://arxiv.org/abs/2010.09885>.

- (14) Wang, S.; Guo, Y.; Wang, Y.; Sun, H.; Huang, J. SMILES-BERT: Large Scale Un-supervised Pre-Training for Molecular Property Prediction. Proceedings of the 10th ACM International Conference on Bioinformatics, Computational Biology and Health Informatics. New York, NY, USA, 2019; p 429–436.
- (15) Kim, S.; Mollaei, P.; Antony, A.; Magar, R.; Farimani, A. B. GPCR-BERT: Interpreting Sequential Design of G Protein Coupled Receptors Using Protein Language Models. 2023; <https://arxiv.org/abs/2310.19915>.
- (16) Guntuboina, C.; Das, A.; Mollaei, P.; Kim, S.; Barati Farimani, A. PeptideBERT: A Language Model Based on Transformers for Peptide Property Prediction. *The Journal of Physical Chemistry Letters* **2023**, *14*, 10427–10434, PMID: 37956397.
- (17) Xu, C.; Wang, Y.; Barati Farimani, A. TransPolymer: a Transformer-based language model for polymer property predictions. *npj Computational Materials* **2023**, *9*, 64.
- (18) Cao, Z.; Magar, R.; Wang, Y.; Barati Farimani, A. MOFormer: Self-Supervised Transformer Model for Metal–Organic Framework Property Prediction. *Journal of the American Chemical Society* **2023**, *145*, 2958–2967.
- (19) Ock, J.; Guntuboina, C.; Barati Farimani, A. Catalyst Energy Prediction with CatBERTa: Unveiling Feature Exploration Strategies through Large Language Models. *ACS Catalysis* **2023**, *13*, 16032–16044.
- (20) Liu, Y.; Ott, M.; Goyal, N.; Du, J.; Joshi, M.; Chen, D.; Levy, O.; Lewis, M.; Zettlemoyer, L.; Stoyanov, V. RoBERTa: A Robustly Optimized BERT Pretraining Approach. 2019; <https://arxiv.org/abs/1907.11692>.
- (21) Liao, Y.-L.; Smidt, T. Equiformer: Equivariant Graph Attention Transformer for 3D Atomistic Graphs. 2023; <https://arxiv.org/abs/2206.11990>.

- (22) Liao, Y.-L.; Wood, B.; Das, A.; Smidt, T. EquiformerV2: Improved Equivariant Transformer for Scaling to Higher-Degree Representations. 2023; <https://arxiv.org/abs/2306.12059>.
- (23) Radford, A.; Kim, J. W.; Hallacy, C.; Ramesh, A.; Goh, G.; Agarwal, S.; Sastry, G.; Askell, A.; Mishkin, P.; Clark, J.; Krueger, G.; Sutskever, I. Learning Transferable Visual Models From Natural Language Supervision. 2021.
- (24) Koot, R.; Hennerbichler, M.; Lu, H. Evaluating Transformers for Lightweight Action Recognition. 2021; <https://arxiv.org/abs/2111.09641>.
- (25) Balaban, M. RTX A6000 Deep Learning Benchmarks. <https://lambdalabs.com/blog/nvidia-rtx-a6000-benchmarks>, 2021; Accessed: 2024-01-01.
- (26) Balaji, S.; Magar, R. GPT-MolBERTa: GPT Molecular Features Language Model for molecular property prediction. 2023; <https://arxiv.org/abs/2310.03030>.
- (27) Xie, T.; Grossman, J. C. Crystal Graph Convolutional Neural Networks for an Accurate and Interpretable Prediction of Material Properties. *Phys. Rev. Lett.* **2018**, *120*, 145301.
- (28) Klicpera, J.; Groß, J.; Günnemann, S. Directional Message Passing for Molecular Graphs. 2020; <https://arxiv.org/abs/2003.03123>.
- (29) Gao, W.; Chen, Y.; Li, B.; Liu, S.-P.; Liu, X.; Jiang, Q. Determining the adsorption energies of small molecules with the intrinsic properties of adsorbates and substrates. *Nature Communications* **2020**, *11*, 1196.
- (30) Esterhuizen, J. A.; Goldsmith, B. R.; Linic, S. Theory-Guided Machine Learning Finds Geometric Structure-Property Relationships for Chemisorption on Subsurface Alloys. *Chem* **2020**, *6*, 3100–3117.

- (31) Hao, Y.; Dong, L.; Wei, F.; Xu, K. Self-attention attribution: Interpreting information interactions inside transformer. Proceedings of the AAAI Conference on Artificial Intelligence. 2021; pp 12963–12971.
- (32) Meidani, K.; Shojaee, P.; Reddy, C. K.; Farimani, A. B. SNIP: Bridging Mathematical Symbolic and Numeric Realms with Unified Pre-training. 2023; <https://arxiv.org/abs/2310.02227>.
- (33) Hammer, B.; Hansen, L. B.; Nørskov, J. K. Improved Adsorption Energetics within Density-Functional Theory using Revised Perdew-Burke-Ernzerhof Functionals. *Phys. Rev. B* **1999**, *59*, 7413–7421.
- (34) Devlin, J.; Chang, M.-W.; Lee, K.; Toutanova, K. BERT: Pre-training of Deep Bidirectional Transformers for Language Understanding. 2019; <https://arxiv.org/abs/1810.04805>.
- (35) van den Oord, A.; Li, Y.; Vinyals, O. Representation Learning with Contrastive Predictive Coding. 2019; <https://arxiv.org/abs/1807.03748>.

Supplementary Information

Hyperparameters and architecture of CatBERTa

Table S1: Overview of CatBERTa’s architecture and training hyperparameters. The CatBERTa encoder retains the same architecture of the publicly available RoBERTa encoder. Identical configurations, except the loss function, are employed in graph-assisted pretraining and the fine-tuning steps.

Hyperparameter	Value
Max positional embeddings	514
Number of attention heads	12
Number of hidden layers	12
Size of each hidden layer	768
Dropout probability in hidden layer	0.1
Batch size	32
Optimizer	AdamW
Scheduler	reduceLR
Initial learning rate	1×10^{-5}
Early stopping threshold	5
Warmup steps	0
Loss function	Cross Entropy or MSE

Results from diverse ML-relaxed structures

Table S2: CatBERTa prediction results from various ML-relaxed structures as generated by GemNet-OC, SCN, and eSCN.

Model	Enhancement	MAE [eV] (\downarrow)			R^2 (\uparrow)		
		GemNet-OC	SCN	eSCN	GemNet-OC	SCN	eSCN
CatBERTa	baseline	0.696	0.720	0.722	0.597	0.584	0.570
	GAP	0.620	0.654	0.656	0.708	0.687	0.679
	CA	0.373	0.382	0.379	0.868	0.862	0.858
	GAP+CA	0.345	0.351	0.341	0.882	0.880	0.883

Prediction results of duplicate text sets

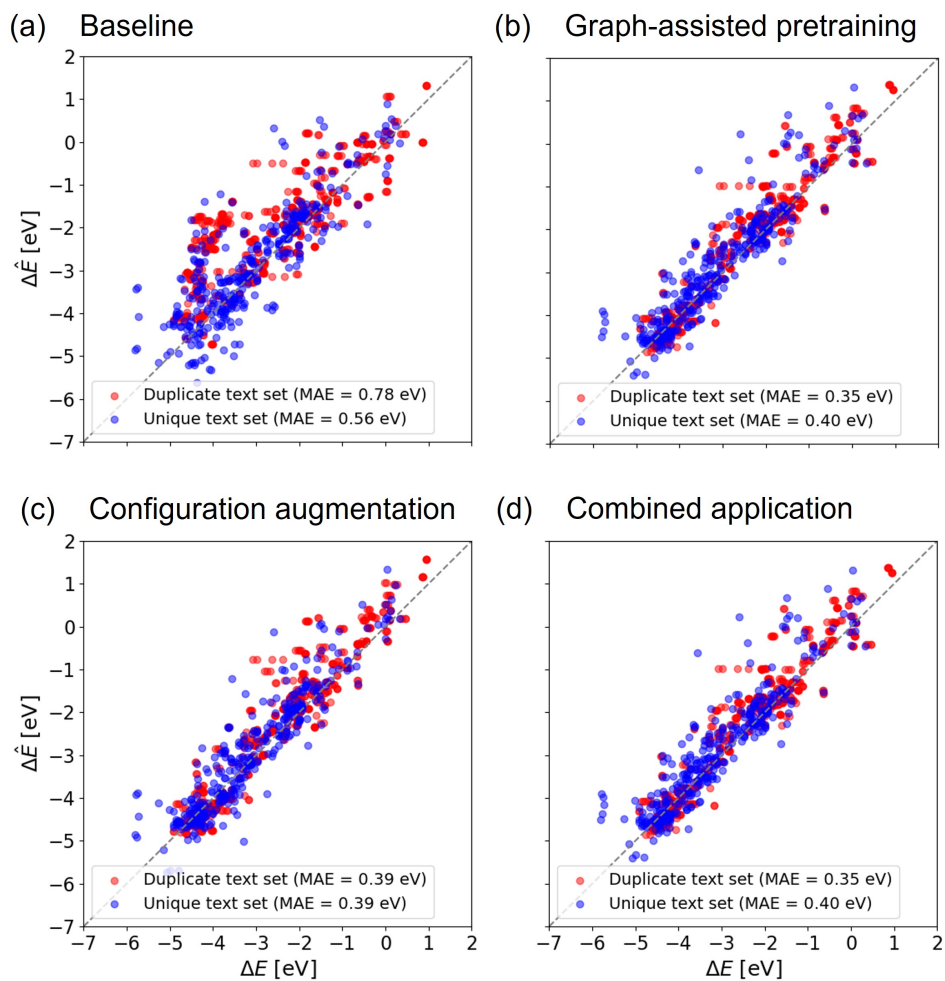


Figure S1: Comparative Parity Plots for Baseline and Enhanced Cases: Duplicate Text Set vs. Unique Text Set Analysis.

